452 J. Med. Chem. 2010, 53, 452–459
DOI: 10.1021/jm901427g

Journal of Medicinal Chemistry Article

Hybrid Inhibitors of Phosphatidylinositol 3-Kinase (PI3K) and the Mammalian Target of Rapamycin (mTOR): Design, Synthesis, and Superior Antitumor Activity of Novel Wortmannin−Rapamycin Conjugates

Semiramis Ayral-Kaloustian,*,† Jianxin Gu,‡ Judy Lucas,§ Michael Cinque,§ Christine Gaydos,§ Arie Zask,† Inder Chaudhary,∥ Jianyao Wang,∥ Li Di,⊥ Mairead Young,⊥ Mark Ruppen,‡ Tarek S. Mansour,† James J. Gibbons,§ and Ker Yu§

†*Discovery Medicinal Chemistry, and* ‡*Preclinical Development, and* §*Discovery Oncology, and* ∥*Drug Metabolism, and* ⊥*Chemical Technologies, Chemical Sciences, Wyeth Research, 401 North Middletown Road, Pearl River, New York 10965*

Received September 24, 2009

Hyperactivation of the PI3K/AKT/mTOR signaling pathway is common in cancer, and PI3K and mTOR act synergistically in promoting tumor growth, survival, and resistance to chemotherapy. Thus, combined targeting of PI3K and mTOR presents an opportunity for robust and synergistic anticancer efficacy. 17-Hydroxywortmannin (**2a**) analogues conjugated to rapamycin (**3a**) analogues via a prodrug linker are uniquely positioned for this approach. Our efforts led to the discovery of diester-linked conjugates that, upon in vivo hydrolysis, released two highly potent inhibitors. Conjugate **7c** provided enhanced solubility relative to **3a** and to an equivalent mixture of **3a** and **9a** and demonstrated profound activity in U87MG mouse xenografts, achieving an MED of 1.5 mg/kg, following weekly intravenous dosing. At 15 mg/kg, **7c** completely inhibited the growth of HT29 tumors, whereas an equivalent mixture of the inhibitors was poorly tolerated. In the A498 renal tumor model, **7c** exhibited superior efficacy over **3a** or **9a** when administered as a single agent or in combination with bevacizumab. Thus, we have uncovered a novel approach to target both PI3K and mTOR via hybrid inhibitors, leading to a broader and more robust anticancer efficacy.

Introduction

The rapamycin analogues (rapalogues) rapamycin, 42-[3-hydroxy-2-(hydroxymethyl)-2-methylpropanoate] (CCI-779, temsirolimus)[1] and 42-*O*-(2-hydroxy)ethyl rapamycin (RAD001, everolimus),[2] are first-in-class mTOR[a] inhibitors approved for cancer therapy. Recent studies indicate that rapalogues are partial inhibitors of mTOR through allosteric binding to mTOR complex-1 (mTORC1) but not mTOR complex-2 (mTORC2), an important player in cancer.[3−5] mTORC1 also negatively regulates the insulin/IGF-1 receptor signaling; thus, blocking of mTORC1 by rapalogues can stimulate PI3K/AKT signaling in some tumors and antagonize its antitumor efficacy.[3,4] This previously unrecognized complexity was investigated in preclinical tumor studies in which treatment with rapamycin (**3a**) or a rapalogue led to increased PI3K activity and AKT signaling, accompanied by minimal inhibition of tumor cell growth.[6,7] In these studies, combination of **3a** with the PI3K inhibitors 2-(4-morpholinyl)-8-phenyl-4*H*-1-benzopyran-4-one (LY294002)[8] or wortmannin (**1**, an irreversible inhibitor with pan-PI3K activity)[9] prevented the rapamycin-induced AKT activation, resulting in a synergistic inhibition of growth.[6,10] It has also been shown that rapalogues induce AKT activation in clinical tumors, which may contribute to resistance to therapy,[11,12] thus pointing to combination therapy with PI3K inhibitors as an avenue to combat such resistance in the clinic.[6,10] In our preclinical studies, we have observed superior in vivo antitumor efficacy by combining minimal doses of the PI3K inhibitor poly(oxy-1,2-ethanediyl)-, α-[2-[[2-[[(1*S*,6b*R*,9*S*,9a*S*,11*R*,11b*R*)-11-(acetyloxy)-1,6,6b,7,8,9,9a,10,11,11b-decahydro-1-(methoxymethyl)-9a,11b-dimethyl-3,6-dioxo-3*H*-furo[4,3,2-*de*]indeno[4,5-*h*]-2-benzopyran-9-yl]oxy]-2-oxoethyl]thio]ethyl]-ω-methoxy- (9CI) (PWT-458),[13] and the mTOR inhibitor PEG-rapamycin.[13] Therefore, these observations collectively identify combination therapy of rapalogues with a PI3K inhibitor as a logical and promising therapeutic strategy.

Wortmannins and rapamycins have been the subject of voluminous research and preclinical and clinical development.[5,13−15] Acetic acid 4-diallylaminomethylene-6-hydroxy-1-α-methoxymethyl-10β,13β-dimethyl-3,7,17-trioxo-1,3,4,7,10,11β,12,13,14α,15,16,17-dodecahydro-2-oxacyclopenta[*a*]phenanthren-11-yl ester (PX-866)[14] is in phase I clinical trials and has been reported to have favorable stability and PK properties relative to other wortmannins. Wortmannin prodrugs and analogues with enhanced stability, solubility, and therapeutic index have been reported by us[16,17] and others.[15] Semisynthetic rapamycin analogues with greater metabolic stability, and improved PK properties compared to **3a** are in various stages of development or approved as drugs.[18−20] Individual leads **9a**[17] and **3a** from these two classes of molecules demonstrate similar potency in target inhibition and similar dose response with

*To whom correspondence should be addressed. Phone: 845-602-4425. Fax: 845-602-5561. E-mail: Ayralks@wyeth.com.

[a] Abbreviations: PI3K, phosphoinositide 3-kinase; mTOR, mammalian target of rapamycin; MED, minimum efficacious dose; mTORC1, mammalian target of rapamycin complex-1; mTORC2, mammalian target of rapamycin complex-2; PEG, polyethlene glycol.

 Published on Web 11/23/2009

intermittent dosing in efficacy models. Therefore, **9a** and **3a** offer a unique opportunity for a combination approach. Furthermore, joining two components, each with its own distinct mechanism of action, into a single novel chemical entity, such as **9a** and **3a** linked via a prodrug linker, can impart enhanced properties or efficacy relative to the equivalent physical combination and improve the therapeutic index, especially relative to **9a** or other wortmannins. Such an entity would also be simpler to use in future drug cocktails for the treatment of cancer. To this end, several novel, covalently linked, cleavable conjugates of the two classes of inhibitors were designed, utilizing the individual inhibitors **9a**, **9b**,[21] **3a**, and **4a**. We describe herein the synthesis, properties, and excellent in vivo efficacy of our conjugates in mouse xenograft models.

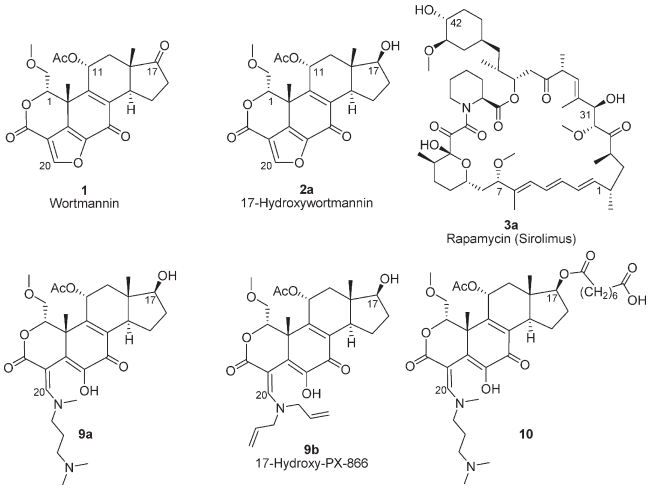

Chemistry

Conjugates **7** and **8** described herein were prepared according to Scheme 1. 17-Hydroxywortmannin (**2a**) was acylated with succinic anhydride, adipic anhydride, or 8-*tert*-butoxy-8-oxooctanoic acid (suberic acid mono-*tert*-butyl ester)[22] to give the corresponding hemiacids (**2b**−**d**). These dicarboxylic acid monoesters were then coupled with the 31-trimethylsilyl rapamycin derivative **3b** or **4b**[23] in the presence of DIPC and DMAP to give the corresponding TMS-protected conjugates. Subsequent deprotection with dilute H_2SO_4 provided the 17,42′-linked wortmannin−rapamycin conjugates **5a**−**c** and **6**. Further treatment of the latter conjugates with *N*,*N*,*N*′-trimethyl-1,3-propanediamine or diallylamine gave the desired furan ring-opened derivatives (**7a**−**d** and **8a**,**b**).

Results and Discussion

The novel conjugates described herein were not active against PI3K or mTOR in the test tube enzyme assays, as expected (data not shown). As described below, in vitro and in vivo stability studies confirmed cleavage of the ester linkers to provide the active moieties, whereupon in vivo efficacy studies were conducted in mouse xenograft models. Representative studies are summarized below.

Stability Studies. In vitro stability studies were conducted via incubation with plasma, whole blood, or liver microsomes of various species. Studies in mouse, rat, and human plasma revealed ester hydrolysis of the linkers. Rates of hydrolyses of the ester moieties were structure and species dependent (plasma stability: human > rat > mouse, as shown for **7c**, Table 1). Conjugates **7a**−**c** had comparable stabilities in female mouse plasma (15%, 4%, and 8% of intact conjugate remaining after 2 h, respectively), whereas **7d** and **8a** appeared more stable, even at 5 h. Addition of sodium fluoride, a known esterase inhibitor, to the mouse plasma suppressed the hydrolysis of conjugates **7a**−**c**, confirming cleavage by esterases.

In female nude mouse blood, the initial ester hydrolysis to give free rapamycin **3a** and the intermediate metabolite, **9a**-suberate monoester (**10**), was fast (Figure 1), and free **9a** was more slowly released from intermediate **10**. As **9a** formed, hydrolysis of the 11-acetyl group was also observed, resulting in the less active metabolite 11-des-Ac-**9a**, reported earlier.[17] Slow release of **9a** from **10** may in part explain the observed enhanced in vivo tolerability for conjugate **7c**, relative to the equivalent physical combination (see Figure 5).

Incubation of **7c** with female nude mouse liver microsomes or mixed human liver microsomes for 30 min, at 37 °C, resulted in moderate metabolism (≥50% **7c** remaining remaining in both, with somewhat less metabolism with human microsomes). The main cleavage observed at 30 min was hydrolysis to give free rapamycin **3a** and the intermediate monoester **10**, via a nonoxidative ester hydrolysis, as evidenced by the lack of dependence on NADPH. In conjunction with the results from 2 h plasma and whole blood studies, these data confirm that the conjugate can be hydrolyzed by esterases, leading to the release of the two active components.

A preliminary study in nude mice, our efficacy species for xenograft studies, dosed at 30 mpk iv, showed hydrolysis of the ester linkers in blood to provide free **9a** and **3a**, confirming the in vitro results.

In Vivo Efficacy Studies. Because we have previously found that the growth of the PTEN-negative U87MG tumors is sensitive to rapamycin and wortmannin analogues, we first tested conjugates **7a**−**c** in this model, using the same low dose of 3 mg/kg (Figure 2). Following a once weekly intravenous (iv) dosing regimen, all three conjugates were highly efficacious. Conjugate **7c**, bearing the suberate linker, was more potent than **7a** or **7b**, bearing the shorter linkers, and exhibited efficacy comparable to that observed with an equivalent physical mixture of **9a** and **3a**. Importantly, similar to the wortmannin analogue **9a**, the conjugate **7c** achieved greatly improved water solubility, whereas **3a** was poorly water-soluble (see below). Thus, an iv formulation of **7c** (and other hybrids) was readily prepared in dextrose−water, whereas **3a**, **4a** (or physical mixtures containing these) required a more complex, less tolerated vehicle (see Experimental Section). In additional studies, **7c** was also more potent than conjugates bearing a less potent wortmannin and/or rapamycin analogue (**9b** and **4a**, respectively), as expected. The potency of **4a** itself was slightly lower than that of **3a**, and a similar trend was observed in conjugate **8b** vs conjugate **7c**, differing only in the rapamycin portion. Wortmannin analogue **9b**[21] was shown to be considerably less potent than **9a**; hence, conjugate **8a** appeared less potent than **8b** and **7c** and higher doses were required to achieve similar efficacy. The rate of hydrolysis of the linkers appears to contribute to the observed potency, where the suberate conjugate **7c** seems to achieve the optimum properties. Keeping the linker constant and changing the active components also affect the rate of cleavage and may in part contribute to the lower in vivo potency of **8a**. Thus, the

nature of the linker (e.g., degree of stability to esterases or contribution to overall properties of the hybrids), as well as the intrinsic potencies of the active moieties, affected the in vivo potencies observed with the conjugates. On the basis of its excellent potency, further studies were conducted with **7c**.

In an antitumor efficacy dose response study, **7c** demonstrated dose dependent inhibition of U87MG tumor growth,

Table 1. Stability of **7c** in the Plasma of Three Species

	amount of **7c** remaining, %		
time (min)	male rat	male human	female mouse
0	100	100	100
5	91	86	53
15	80	93	39
30	71	91	18
60	64	83	13
90	53	82	10
120	46	83	8

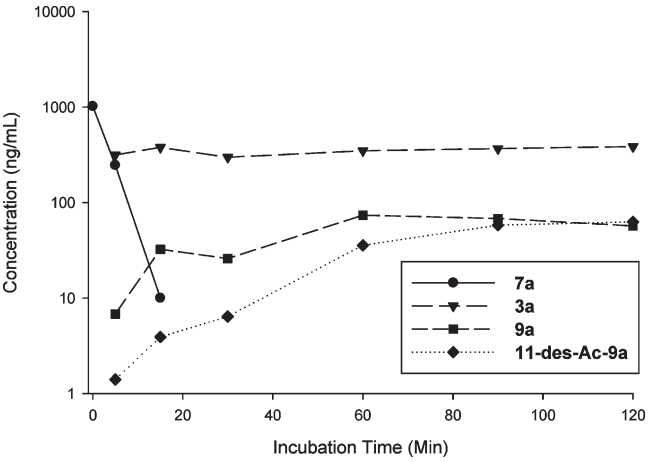

Figure 1. Cleavage of **7c** in nude mouse blood: slow release of **9a**, followed by formation of 11-des-Ac-**9a**.

Scheme 1. Synthesis of 17,42′ Linked Wortmannin−Rapamycin Conjugates[a]

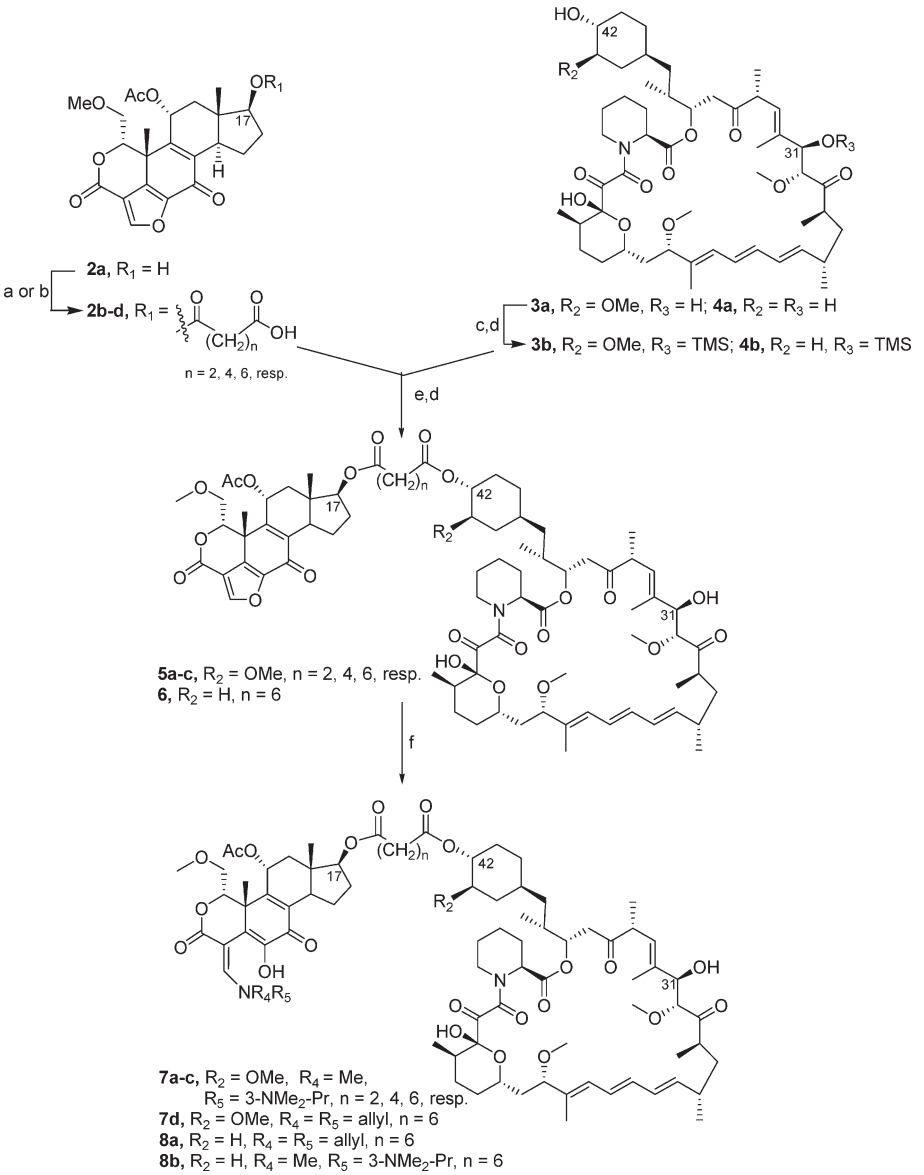

[a] Reagents and conditions: (a) succinic anhydride ($n = 2$) or adipic anhydride ($n = 4$), DCC, DMAP; (b) (1) suberic acid mono-*tert*-butyl ester, DCC, DMAP; (2) HCl, AcOH; (c) TMSCl, imidazole; (d) 0.5 N H_2SO_4; (e) DIPC, DMAP; (f) HNR_4R_5.

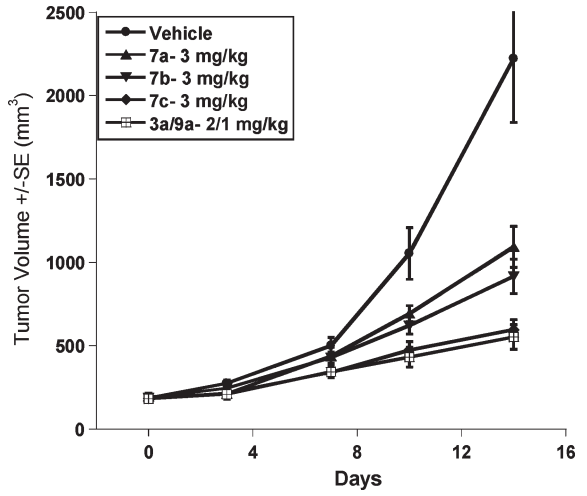

Figure 2. Antitumor activity of **7a**−**c** and a physical mixture of **3a** and **9a** in the xenograft glioma model. U87MG tumors were grown in nude mice and were staged and randomized to treatment groups (n = 10). The conjugates **7a**, **7b**, and **7c** (3 mg/kg) or a physical mixture of **3a** (2 mg/kg) and **9a** (1 mg/kg) were dosed to mice intravenously (iv) once weekly (days 0, 6, 13). Tumor growth was monitored twice a week, and tumor volume was determined as described.[13]

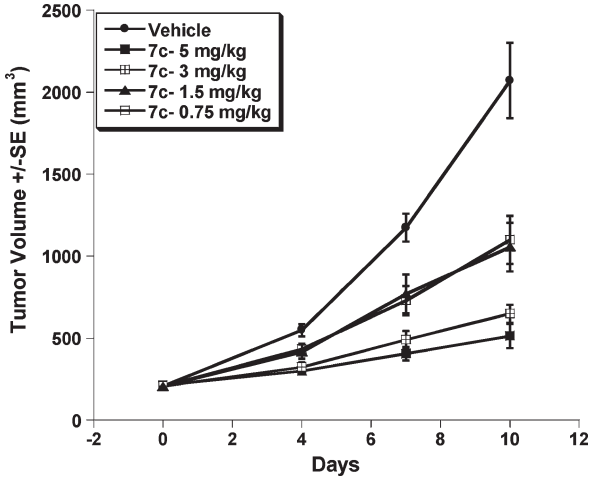

Figure 3. Dose response of **7c** in inhibition of U87MG tumor growth. U87MG tumor-bearing mice (n = 10) were dosed iv once weekly with vehicle or **7c** at 5, 3, 1.5, and 0.75 mg/kg (days 0, 6).

achieving an MED of approximately 0.75−1.5 mg/kg iv (Figure 3) dosed once per week. A 5 mg/kg dose was slightly more effective than a 3 mg/kg dose.

In order to assess the effect of **7c** on AKT phosphorylation, the conjugate was dosed once at 15 mg/kg to U87MG tumor bearing mice, and tumors excised at 2 h after treatment were subjected to Western blot analysis (Figure 4). In comparison to vehicle-treated controls, **7c** strongly inhibited phosphorylation of AKT both at S473 (mTORC2 inhibition) and at T308 (PI3K inhibition), whereas an equivalent dose of **3a** (10 mg/kg) had no effect. As expected, the mTORC2 biomarker pS6K was inhibited by both **3a** and conjugate **7c**. Actin protein, used as a control, was not affected. This result confirms that a conjugate such as **7c** can overcome AKT activation and/or resistance to therapy, as observed with rapalogues,[10−12] and effectively knock down AKT phosphorylation.

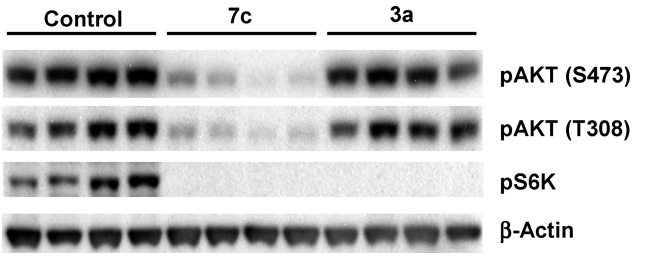

Figure 4. In vivo inhibition of AKT phosphorylation by **7c**, 2 h after dosing at 15 mg/kg iv, in the U87MG mouse xenogrgaft model. Compound **3a** was dosed at 10 mg/kg.

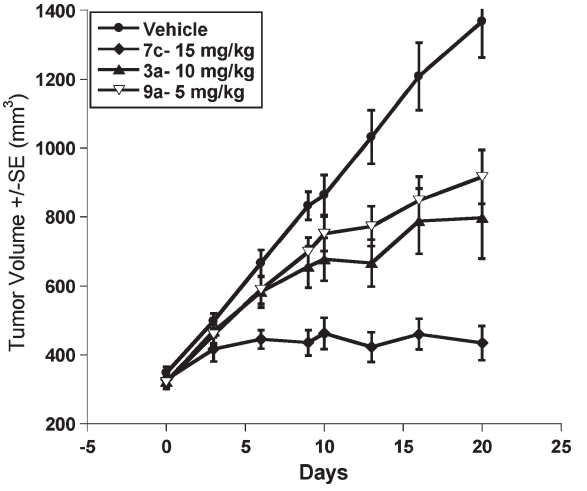

Figure 5. Antitumor activity of **7c** in the HT29 colon tumor model. HT29 tumor-bearing mice (n = 10) were dosed iv once weekly with vehicle, **7c** at 15 mg/kg, **3a** at 10 mg/kg, **9a** at 5 mg/kg. A physical combination of **3a** and **9a** at the indicated dosages was not tolerated (data not shown).

We next evaluated **7c** in HT29, a colon tumor model that is not exquisitely sensitive to rapamycin or wortmannin analogues. At 15 mg/kg, **7c** completely inhibited the growth of HT29 colon tumors, compared to the partial inhibition elicited by 5 mg/kg **9a** or 10 mg/kg **3a** (Figure 5). However, an equivalent physical mixture of the individual inhibitors **9a** and **3a** at these doses was poorly tolerated (data not shown). As mentioned earlier, compound **3a** was very poorly soluble in water (2.6 μg/mL)[24] and required a complex formulation for iv administration. Conjugation of **3a** (or **4a**) to the soluble open-ring wortmannin derivative **9a** or **9b** (solubility at pH 7.4: >10 mg/mL[17] and >100 μg/mL, respectively) provided single agents with greatly enhanced water solubility (solubility of **7c** in water: 460 μg/mL) relative to the rapamycins or the physical mixture of the two active moieties. This, in addition to the slow release of the wortmannin component, may contribute to the enhanced tolerability of conjugate **7c** (Figure 5), relative to the physical mixture.

Since rapalogues temsirolimus and everolimus have been used clinically for treating renal cancers, we compared **7c** with **3a** in the A498 renal tumor model. At 30 mg/kg iv, **7c** exhibited superior antitumor efficacy relative to 25 mg/kg **3a** when administered as a single agent (Figure 6; compare the left and right graphs). Furthermore, **7c**, in combination with bevacizumab, achieved a substantial regression of larger A498 tumors (Figure 6, right graph). In contrast, dramatic tumor regression was not demonstrated by the combination of **3a** with bevacizumab (Figure 6, left graph).

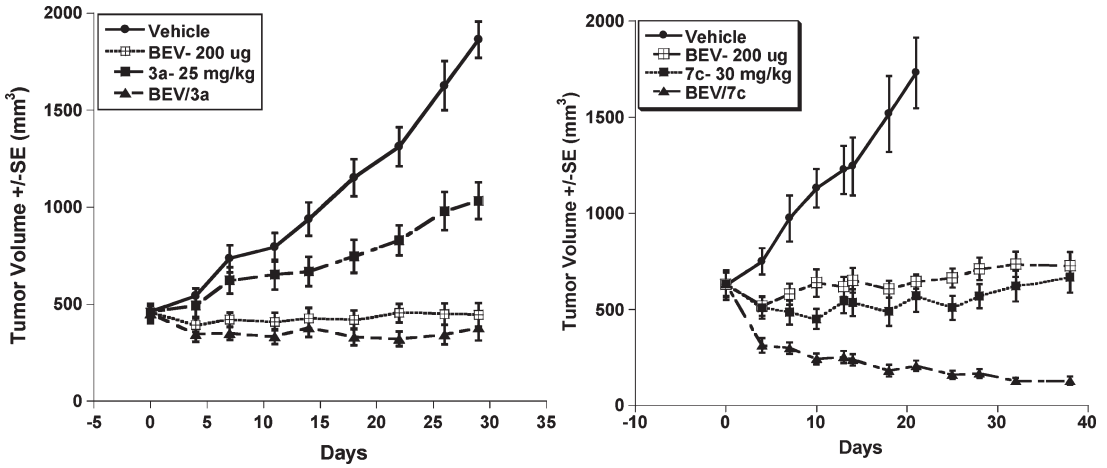

Figure 6. **7c** is more efficacious than **3a** in the renal tumor model. Left graph: A498 tumor-bearing mice (n = 10) were dosed iv once weekly with vehicle, **3a** at 25 mg/kg, bevacizumab (BEV) at 200 μg per mouse, or the combination of **3a** and bevacizumab. Right graph: A498 tumor-bearing mice were similarly dosed iv with vehicle, **7c** at 30 mg/kg, bevacizumab, or the combination of **7c** and bevacizumab.

Conclusions

The strategy of hitting multiple targets via hybrid molecules or conjugates has recently gained popularity.[25,26] A cleavable conjugate of two drugs, each of which can effectively and independently hit its respective target, can afford new opportunities to enhance efficacy in a wider range of tumors or provide a better therapeutic index. We envisioned this approach as a novel and effective way to use rapamycins for oncology and to attenuate the metabolic or toxicity liabilities of certain wortmannin analogues. This led to the discovery of a series of novel diester-linked 17-hydroxywortmannin/rapamycin conjugates, **7a**−**d** and **8a**,**b**, which upon in vivo hydrolysis release two highly potent inhibitors of PI3K and mTOR. Conjugation confers enhanced water solubility relative to rapamycins and relative to an equivalent mixture of the two active moieties. As demonstrated for conjugate **7c**, the enhanced solubility and slower, more steady release of the wortmannin component **9a** provides enhanced tolerability relative to the physical combination of **9a** and **3a** and excellent in vivo efficacy in xenograft models, both as a single agent or in combination with bevacizumab. Thus, we have uncovered a novel approach to target both PI3K and mTOR with a single chemical entity that can release two very potent inhibitors, leading to a broader and more robust anticancer efficacy. Such an entity would also be simpler to use in drug cocktails for the treatment of cancer. Linkers may be further modified or specific analogues of wortmannin or rapamycin can be selected to further improve properties or efficacy of the conjugates.

Experimental Section

Nude Mouse Xenograft Efficacy and Biomarker Studies. Cell lines of U87MG, HT29, and A498 were obtained from American Type Culture Collection (ATCC). All cells were cultured using standard cell culture methods. For efficacy experiments, nude mice bearing U87MG, HT29, and A498 tumors were randomized into treatment groups (n = 10). The conjugates and the 17-hydroywortmannin analogue **9a** were formulated in 5% dextrose in water (D5W). Rapamycin **3a** and its physical combination with **9a** were formulated in a vehicle containing 4% ethanol, 5% polysorbate 80, 5% polyethylene glycol (PEG)-400. Tumor-bearing mice were dosed intravenously (iv), using a once weekly regimen at the indicated dosages. Avastin (bevacizumab) was formulated in phosphate-buffered saline (PBS) and dosed intraperitoneally (ip) once weekly. Tumor growth was monitored and analyzed as described previously.[13] In vivo biomarker studies with U87MG tumors were conducted as described previously.[13]

In Vitro Plasma, Whole Blood, and Microsomal Stability Studies.

In Vitro Stability in Plasma of Mice, Rat, and Human. Hydrolysis kinetics of **7c** was determined in vitro in plasma at 37 °C for 2 h with anticoagulent (heparin). Plasma samples were collected at various time points quenched with acetonitrile (3×). The supernatant was transferred to clean tubes, dried under nitrogen, and reconstituted in methanol and water (20:80). An aliquot of reconstituted extract was injected onto LC/MS for determination of concentrations of **7c**. Further degradation products, **3a**, **9a**, and 11-des-Ac-**9a** were determined by mass spectrometry.

In Vitro Stability in Nude Mouse Whole Blood. Hydrolysis kinetics of **7c** was determined in vitro in plasma and whole blood at 37 °C for 2 h with different anticoagulents (heparin and sodium flouride/EDTA. Plasma or whole blood samples were collected at various time points quenched with acetonitrile (3×). The supernatant was transferred to clean tubes, dried under nitrogen, and reconstituted in methanol and water (20:80). An aliquot of reconstituted extract was injected onto LC/MS for determination of concentrations of **7c**, **3a**, **9a**, and 11-des-Ac-**9a**.

In Vitro Stability in Hepatic Microsomes. To evaluate the mechanism of hybrid inhibitor, **7c** (10 μM) was incubated for 30 min at 37 °C in various media including buffer (pH 7.4), boiled human liver microsomes (1 mg/mL), and native human liver microsomes (1 mg/mL). At the end of incubation, the incubation was quenched by addition of 3-fold (by volume) of cold acetonitrile. The supernatants were transferred to clean tubes, dried under nitrogen, and reconstituted in 300 μL of 20:80 MeOH/H_2O (v/v). An aliquot (50 μL) of the reconstituted extract was injected onto LC/MS for analysis.

Chemistry. General Methods. ^{1}H and ^{13}C NMR NMR spectra were recorded on a Bruker AV300 or a Bruker AV400 spectrometer, in the indicated solvent, using TMS as the internal standard. In solution, rapalogues exist as a mixture of amide rotamers (~4:1 ratio for rapamycin[27]). The ^{13}C data reported for compounds containing a rapamycin moiety are for the major rotamer only. All HRMS data were obtained on a Bruker APEXII FTICR mass spectrometer equipped with Bruker APOLLO ESI source. Analytical HPLC were recorded on a Waters 2690 instrument: column, YMC ODS-AQ12S03-1546WT, 150 mm × 4.6 mm; mobile phase, 70−90% B in 15 min, then to 95% B in 25 min (mobile phase A = 5 mM EDTA, B = MeOH); flow rate, 0.6 mL/min; column temp, 27 °C; wavelength, 254 nm. The purity of all compounds was ≥95%

based on analytical HPLC. When compounds contained a rapamycin moiety, the HPLC purity was based on the combined B (pyran form) and C (oxepane form) hemiketal isomers[28] formed at C-13 vs C-15, respectively (with pyran form major).

Compounds **2a**, **3a**, and **4a** were obtained in-house.

(1*E*,4*S*,4a*R*,5*R*,6a*S*,7*S*)-5-(Acetyloxy)-1-{[[3-(dimethylamino)-propyl](methyl)amino]methylene}-11-hydroxy-4-(methoxymethyl)-4a,6a-dimethyl-2,10-dioxo-1,2,4,4a,5,6,6a,7,8,9,9a,10-dodecahydro-indeno[4,5-*h*]isochromen-7-yl-(1*R*,2*R*,4*S*)-4-{(2*R*)-2-[(3*S*,6*R*,7*E*,9*R*,10*R*,12*R*,14*S*,15*E*,17*E*,19*E*,21*S*,23*S*,26*R*,27*R*,34a*S*)-9,27-dihydroxy-10,21-dimethoxy-6,8,12,14,20,26-hexamethyl-1,5,11,28,29-pentaoxo-1,4,5,6,9,10,11,12,13,14,21,22,23,24,25,26,27,28,29,31,32,33,34,34a-tetracosahydro-3*H*-23,27-epoxypyrido[2,1-*c*][1,4]oxazacyclohentriacontin-3-yl]propyl}-2-methoxycyclohexyl Succinate (7a). To a solution of (1*S*,9*S*,9a*S*,11*R*,11b*R*)-9-hydroxy-1-(methoxymethyl)-9a,11b-dimethyl-3,6-dioxo-3,6,6b,7,8,9,9a,10,11,11b-decahydro-1*H*-furo[4,3,2-*de*]indeno[4,5-*h*]isochromen-11-yl acetate (**2a**, 430 mg, 1 mmol) in CH_2Cl_2 (10 mL) was added succinic anhydride (250 mg, 2.5 mmol), followed by DMAP (244 mg, 2 mmol). The mixture was then stirred at room temperature overnight. The crude material was purified on a silica gel column, eluting with hexane/acetone to give 4-((1*S*,9*S*,9a*S*,11*R*,11b*R*)-11-acetoxy-1-(methoxymethyl)-9a,11b-dimethyl-3,6-dioxo-3,6,6b,7,8,9,9a,10,11,11b-decahydro-1*H*-furo[4,3,2-*de*]indeno[4,5-*h*]isochromen-9-yloxy)-4-oxobutanoic acid (**2b**, 470 mg) as a white powder. MS (ESI) m/z 553 $(M + Na)^+$.

A mixture of **2b** (795 mg, 1.5 mmol), 31-trimethylsilyl rapamycin (**3b**, 1.18 g, 1.2 mmol),[23] and a catalytic amount of DMAP (73 mg, 0.6 mmol) in 1,2-dichloroethane (10 mL) was cooled to 0−5 °C and was treated with 1,3-diisopropylcarbodiimide (302 mg, 2.4 mmol). The mixture was stirred at 0−5 °C for 3 h, then warmed to room temperature and stirred for 12 h. The mixture was then loaded on a silica gel pad (30 g, 60 Å, 230−400 mesh). The pad was eluted first with hexane/EtOAc (2:1, 200 mL), then with hexane/EtOAc (3:2, 50 mL), and finally with hexane/EtOAc(1:1, 250 mL). The fraction that contained the product eluted with hexane/EtOAc (1:1) was concentrated under reduced pressure. The resulting crude product (1.6 g) was dissolved in MeCN (15 mL), cooled to 0−5 °C, and treated with 0.5 N H_2SO_4 (12 mL) for 2 h. Ethyl acetate was added, and the organic layer was separated. The organic layer was washed with water, 5% $NaHCO_3$, and brine and dried. After the solvent was evaporated in vacuo, the crude residue was purified on a silica gel column, eluting with hexane/acetone to give the desired product **5a** as a white foam. HRMS (ESI) m/z calcd for $C_{78}H_{107}NO_{23}$ ($[M + Na]^+$) 1448.7126, found 1448.7137. HPLC analysis showed >99% purity (total of B + C isomers).[28]

A solution of **5a** (250 mg, 0.175 mmol) in TBME (7 mL) was cooled to −30 to −35 °C and treated with a solution of *N*,*N*,*N*′-trimethyl-1,3-propanediamine (23 mg mg, 0.2 mmol) in TBME (1 mL) over 10 min. The mixture was stirred for 30 min at −30 °C, then slowly warmed to −20 °C and stirred at −20 °C for another 1 h. Hexane (8 mL) was then introduced while maintaining the temperature at −15 to −20 °C. After the mixture was stirred for 10 min, the precipitates were collected on a Buchner funnel, washed with cold hexane/TBME (1:0.8), and dried in vacuo. The product (**7a**) was obtained as a yellow powder (182 mg, 67%). HRMS (ESI), m/z calcd for $C_{84}H_{124}N_3O_{23}$ ($[M + H]^+$) 1542.8620, found 1542.8610; ^{1}H NMR ($CDCl_3$, 300 MHz, representative data) δ 8.14 (s, 1H), 6.43−5.87 (m, 5H), 5.59−5.11 (m, 4H), 4.87−4.17 (m, 5H), 3.92−3.55 (m, 5H), 3.41−3.11 (m, 21H), 2.82−2.45 (m, 14H), 2.36−1.90 (m, 20H); ^{13}C NMR ($CDCl_3$, 100 MHz, representative data) δ 215.0, 208.1, 192.8, 179.0, 172.1, 171.7, 169.8, 169.2, 166.7, 150.0, 140.0, 137.6, 136.1, 135.7, 133.5, 130.2, 129.6, 126.8, 98.5, 88.2, 84.7, 84.2, 82.5, 80.8, 77.3, 76.7, 75.4, 73.2, 69.1, 67.1, 59.3, 59.2, 58.5, 57.5, 55.9, 51.3, 46.6, 45.4, 44.5, 44.2, 42.9, 42.7, 41.6, 41.5, 40.6, 40.2, 39.0, 38.3, 36.0, 35.1, 33.8, 33.2, 32.9, 31.2, 29.7, 29.4, 29.2, 27.7, 27.2, 27.0, 25.7, 25.3, 24.3, 21.6, 21.4, 21.1, 20.7, 16.2, 16.0, 15.9, 14.9, 13.7, 13.9, 13.2, 10.2.

(1*E*,4*S*,4a*R*,5*R*,6a*S*,7*S*)-5-(Acetyloxy)-1-{[[3-(dimethylamino)-propyl](methyl)amino]methylene}-11-hydroxy-4-(methoxymethyl)-4a,6a-dimethyl-2,10-dioxo-1,2,4,4a,5,6,6a,7,8,9,9a,10-dodecahydro-indeno[4,5-*h*]isochromen-7-yl-(1*R*,2*R*,4*S*)-4-{(2*R*)-2-[(3*S*,6*R*,7*E*,9*R*,10*R*,12*R*,14*S*,15*E*,17*E*,19*E*,21*S*,23*S*,26*R*,27*R*,34a*S*)-9,27-dihydroxy-10,21-dimethoxy-6,8,12,14,20,26-hexamethyl-1,5,11,28,29-pentaoxo-1,4,5,6,9,10,11,12,13,14,21,22,23,24,25,26,27,28,29,31,32,33,34,34a-tetracosahydro-3*H*-23,27-epoxypyrido[2,1-*c*][1,4]oxazacyclohentriacontin-3-yl]propyl}-2-methoxycyclohexyl Hexanedioate (7b). A solution of adipic acid (1.75 g, 12 mmol) in acetic anhydride (5 mL) was heated at reflux for 1.5 h. The mixture was then concentrated under reduced pressure and chased with toluene (4 × 30 mL) and MeCN (30 mL). The crude adipic anhydride was then reacted with **2a**, following the procedure used for **2b**, to get 4-((1*S*,9*S*,9a*S*,11*R*,11b*R*)-11-acetoxy-1-(methoxymethyl)-9a,11b-dimethyl-3,6-dioxo-3,6,6b,7,8,9,9a,10,11,11b-decahydro-1*H*-furo[4,3,2-*de*]indeno[4,5-*h*]-isochromen-9-yloxy)-6-oxohexanoic acid (**2c**, 835 mg) as a white powder. MS (ESI) m/z 559 $(M + H)^+$.

Following the procedure for **5a**, compound **2c** (680 mg, 1.22 mmol) was reacted with 31-trimethylsilyl rapamycin (**3b**, 986 mg, 1 mmol),[23] and the resulting trimethylsilyl intermediate (1.2 g) was treated with H_2SO_4 (0.5 N, 9 mL) to yield the desired product **5b** as a white foam, after purification. HRMS (ESI) m/z calcd for $C_{80}H_{111}NO_{23}$ ($[M + Na]^+$) 1476.7439, found 1476.7438. HPLC analysis showed 96.6% purity (B + C isomers).

Compound **5b** (250 mg, 0.172 mmol) was treated with *N*,*N*,*N*′-trimethyl-1,3-propanediamine (23 mg, 0.2 mmol), according to the procedure for **7a**, to provide the desired conjugate **7b** as a yellow powder (175 mg, 65%). HRMS (ESI) m/z calcd for $C_{86}H_{128}N_3O_{23}$ ($[M + H]^+$) 1570.8933, found 1570.8925; ^{1}H NMR ($CDCl_3$, 300 MHz, representative data) δ 8.14 (s, 1H), 6.43−5.11 (m, 9H), 4.86−4.17 (m, 5H), 3.90−3.11 (m, 28H); ^{13}C NMR ($CDCl_3$, 100 MHz, representative data) δ 215.0, 208.2, 192.9, 179.1, 173.2, 172.8, 169.9, 169.3, 166.8, 150.0, 140.0, 137.6, 136.1, 135.8, 133.5, 130.2, 129.4, 126.5, 98.5, 88.2, 84.8, 84.3, 82.6, 80.9, 80.4, 77.3, 76.1, 75.4, 73.2, 69.2, 67.2, 59.4, 59.2, 58.5, 57.4, 55.9, 55.9, 51.3, 49.4, 46.6, 45.4, 44.4, 44.2, 43.0, 42.7, 41.6, 41.5, 40.6, 40.2, 39.0, 38.4, 36.0, 35.1, 34.2, 34.0, 33.8, 33.3, 32.9, 31.3, 31.2, 29.8, 27.8, 27.2, 27.0, 25.7, 25.3, 24.4, 24.3, 21.5, 21.2, 20.7, 16.2, 16.0, 13.7, 13.4, 13.3, 10.2.

(1*E*,4*S*,4a*R*,5*R*,6a*S*,7*S*)-5-(Acetyloxy)-1-{[[3-(dimethylamino)-propyl](methyl)amino]methylene}-11-hydroxy-4-(methoxymethyl)-4a,6a-dimethyl-2,10-dioxo-1,2,4,4a,5,6,6a,7,8,9,9a,10-dodecahydro-indeno[4,5-*h*]isochromen-7-yl-(1*R*,2*R*,4*S*)-4-{(2*R*)-2-[(3*S*,6*R*,7*E*,9*R*,10*R*,12*R*,14*S*,15*E*,17*E*,19*E*,21*S*,23*S*,26*R*,27*R*,34a*S*)-9,27-dihydroxy-10,21-dimethoxy-6,8,12,14,20,26-hexamethyl-1,5,11,28,29-pentaoxo-1,4,5,6,9,10,11,12,13,14,21,22,23,24,25,26,27,28,29,31,32,33,34,34a-tetracosahydro-3*H*-23,27-epoxypyrido[2,1-*c*][1,4]oxazacyclohentriacontin-3-yl]propyl}-2-methoxycyclohexyl Octanedioate (7c). A solution of **2a** (4.30 g, 10 mmol) and 8-*tert*-butoxy-8-oxooctanoic acid (suberic acid mono-*tert*-butyl ester; 2.70 g, 11.74 mmol)[22] in MeCN (40 mL) was cooled to 0−5 °C, and DMAP (61 mg, 0.5 mmol) was added, followed by DCC (2.60 g, 12.6 mmol). The mixture was stirred at 0 °C for 6 h and then warmed to room temperature and stirred for 12 h. The white precipitate was removed by filtration and washed with 2 × 10 mL of MeCN. The filtrate was then added to H_2O (160 mL) while stirring. The solid was collected on a Buchner funnel and washed first with cold *i*-PrOH (2 × 20 mL), then hexane (2 × 20 mL), and dried in vacuo (5.6 g, 87%). The above solid was dissolved in 1 M HCl in AcOH (40 mL) and stirred at room temperature for 4 h. Water (150 mL) was added. The solid was collected on a Buchner funnel and washed with water (3 × 30 mL). The wet cake was then dissolved in acetone (35 mL), and water (120 mL) was added dropwise over 10 min, while stirring. The precipitated solid was collected and washed with water

(30 mL), then dried in vacuo at 50 °C for 24 h. 8-((1*S*,9*S*,9a*S*,11*R*,11b*R*)-11-Acetoxy-1-(methoxymethyl)-9a,11b-dimethyl-3,6-dioxo-3,6,6b,7,8,9,9a,10,11,11b-decahydro-1*H*-furo[4,3,2-*de*]indeno[4,5-*h*]isochromen-9-yloxy)-8-oxooctanoic acid, **2d**, was obtained as a white powder (5.0 g, 97%). MS (ESI) *m*/*z* 609 (M + Na); ^{1}H NMR ($CDCl_3$, 300 MHz) δ 10.35 (br, 1H), 8.19 (s, 1H), 6.08−6.03 (m,1H), 4.82−4.74 (m, 2H), 3.45−3.41 (m, 1H), 3.15 (s, 3H), 2.98−2.94 (m, 1H), 2.8−2.77 (m, 1H), 2.61−2.56 (m, 1H), 2.50−2.43 (m, 1H), 2.34−2.26 (m, 4H), 2.10 (s, 3H), 2.07−2.05 (m, 2H), 1.74−1.33 (m, 14H), 0.85 (s, 3H); ^{13}C NMR ($CDCl_3$, 75 MHz) δ 179.72, 174.07, 173.19, 170.12, 158.10, 150.32, 148.96, 145.28, 143.03, 141.67, 114.51, 89.25, 79.99, 73.21, 70.80, 59.75, 45.04, 44.40, 41.02, 40.52, 34.61, 34.24, 29.06, 29.00, 27.85, 26.89, 25.10, 25.05, 24.82, 21.49, 13.22.

Reaction of **2d** (5.86 g, 10 mmol), with **3b** (7.89 g, 8 mmol), followed by hydrolysis of the intermediate trimethylsilyl ether, according to the procedure above for **5a**, gave the desired product **5c** as a white foam (8.5 g, 72%). HRMS (ESI) *m*/*z* calcd for $C_{82}H_{115}NO_{23}$ ([M + Na]$^+$) 1504.7752, found 1504.7755. HPLC analysis showed >99% purity (B + C isomers).

A solution of **5c** (7.80 g, 5.26 mmol) in TBME (250 mL) was treated with *N*,*N*,*N*′-trimethyl-1,3-propanediamine (700 mg, 6 mmol) as before for **7a**, to yield **7c** as a yellow powder (7.95 g, 94%). HRMS (ESI) *m*/*z* calcd for $C_{88}H_{132}N_3O_{23}$ ([M + H]$^+$) 1598.9246, found 1598.9234; ^{1}H NMR ($CDCl_3$, 300 MHz, representative data) δ 8.14 (s, 1H), 6.43−5.87 (m, 5H), 5.59−5.11 (m, 4H), 4.86−4.18 (m, 5H), 3.90−3.11 (m, 27H); 2.75−2.23 (m, 24H); ^{13}C NMR ($CDCl_3$, 100 MHz, representative data) δ 215.0, 208.2, 192.8, 179.1, 173.6, 173.2, 169.9, 169.3, 166.7, 150.0, 140.0, 137.7, 136.1, 135.7, 133.5, 130.2, 129.4, 126.5, 98.5, 88.3, 84.8, 84.3, 82.6, 80.9, 80.3, 77.3, 76.0, 75.5, 73.2, 69.2, 67.2, 59.4, 59.2, 58.5, 57.5, 56.0, 51.3, 49.4, 46.6, 45.3, 44.4, 44.2, 43.0, 42.0, 41.6, 41.5, 40.6, 40.2, 39.0, 38.4, 36.0, 35.1, 35.0, 34.3, 33.8, 33.3, 32.8, 31.3, 31.2, 29.8, 28.8, 28.7, 27.8, 27.2, 27.0, 25.7, 25.3, 24.8, 24.8, 24.3, 21.5, 21.2, 20.7, 16.2, 16.0, 15.9, 13.7, 13.4, 13.2, 10.2.

(1*E*,4*S*,4a*R*,5*R*,6a*S*,7*S*)-5-Acetyloxy-1-[(diallylamino)methylene]-11-hydroxy-4-(methoxymethyl)-4a,6a-dimethyl-2,10-dioxo-1,2,4,4a,5,6,6a,7,8,9,9a,10-dodecahydroindeno[4,5-*h*]isochromen-7-yl-(1*R*,2*R*,4*S*)-4-{(2*R*)-2-[(3*S*,6*R*,7*E*,9*R*,10*R*,12*R*,14*S*,15*E*,17*E*,19*E*,21*S*,23*S*,26*R*,27*R*,34a*S*)-9,27-dihydroxy-10,21-dimethoxy-6,8,12,14,20,26-hexamethyl-1,5,11,28,29-pentaoxo-1,4,5,6,9,10,11,12,13,14,21,22,23,24,25,26,27,28,29,31,32,33,34,34a-tetracosahydro-3*H*-23,27-epoxypyrido[2,1-*c*][1,4]oxazacyclohentriacontin-3-yl]propyl}-2-methoxycyclohexyl Octanedioate (7d). A solution of **5c** (1.0 g, 0.67 mmol) in TBME (30 mL) was cooled in an ice bath and treated with diallylamine (0.15 mL) for 48 h and then concentrated to a volume of about 10 mL and triturated with hexane (50 mL). The product (**7d**) was collected on a Buchner funnel as a yellow powder (985 mg, 92%). HRMS (ESI) *m*/*z* calcd for $C_{88}H_{126}N_2O_{23}$ ([M + Na]$^+$) 1601.8644, found 1601.8637; ^{1}H NMR ($CDCl_3$, 300 MHz, representative data) δ 8.14 (s, 1H), 6.82 (br, 1H), 6.43−5.83 (m, 6H), 5.58−5.10 (m, 9H), 4.86−4.18 (m, 5H), 3.96−3.11 (m, 26H), 2.75−2.28 (m, 13H), 2.10−0.81 (m, 65H); ^{13}C NMR ($CDCl_3$, 100 MHz, representative data) δ 215.0, 208.2, 192.8, 179.0, 173.6, 173.2, 169.8, 169.3, 166.8, 150.6, 139.9, 139.4, 137.5, 136.1, 135.8, 133.5, 130.2, 129.4, 126.4, 119.4, 98.5, 89.1, 84.8, 84.2, 82.5, 80.9, 80.2, 77.1, 76.0, 75.4, 73.1, 69.3, 67.2, 59.4, 59.1, 57.5, 55.9, 55.9, 51.3, 49.4, 46.6, 44.4, 44.2, 43.0, 42.7, 41.5, 40.6, 40.2, 39.0, 38.4, 36.0, 35.1, 34.6, 34.3, 33.8, 33.3, 32.9, 31.3, 31.2, 29.8, 28.8, 28.7, 27.8, 27.2, 27.0, 25.3, 24.8, 24.3, 21.4, 21.2, 20.7, 16.2, 16.0, 15.9, 13.6, 13.4, 13.3, 10.2.

(1*E*,4*S*,4a*R*,5*R*,6a*S*,7*S*)-5-Acetyloxy-1-[(diallylamino)methylene]-11-hydroxy-4-(methoxymethyl)-4a,6a-dimethyl-2,10-dioxo-1,2,4,4a,5,6,6a,7,8,9,9a,10-dodecahydroindeno[4,5-*h*]isochromen-7-yl-*trans*-4-{(2*R*)-2-[(3*S*,6*R*,7*E*,9*R*,10*R*,12*R*,14*S*,15*E*,17*E*,19*E*,21*S*,23*S*,26*R*,27*R*,34a*S*)-9,27-dihydroxy-10,21-dimethoxy-6,8,12,14,20,26-hexamethyl-1,5,11,28,29-pentaoxo-1,4,5,6,9,10,11,12,13,14,20,26-hexamethyl-1,5,11,28,29-pentaoxo-1,4,5,6,9,10,11,12,13,14,21,22,23,24,25,26,27,28,29,31,32,33,34,34a-tetracosahydro-3*H*-23,27-epoxypyrido[2,1-*c*][1,4]oxazacyclohentriacontin-3-yl]propyl}cyclohexyl Octanedioate (8a). Following the procedure above for the synthesis of **5a**, reaction of **2d** (0.92 g, 1.57 mmol) with 31-trimethylsilyl 41-desmethoxyrapamycin (**4b**, 1.20 g, 1.26 mmol, prepared according to the procedure for **3b**)[23] provided the 31-trimethylsilyl intermediate. Hydrolysis of the 31-trimethylsilyl ether, followed by workup and silica gel purification as before, provided the desired intermediate **6** as a white foam (1.54 g, 84%). HRMS (ESI) *m*/*z* calcd for $C_{81}H_{113}NO_{22}$ ([M + Na]$^+$) 1474.7646, found 1474.7646. HPLC analysis showed 98% purity (B + C isomers).

Diallylamine (64 mg, 0.66 mmol) was added to an ice-cold solution of **6** (552 mg, 0.38 mmol) in TBME (15 mL). The mixture was then stirred at 0 °C for 40 h. The resulting mixture was concentrated to about 5 mL in vacuo and then triturated with hexane (30 mL). The product **8a** was collected on a Buchner funnel as a yellow powder (540 mg, 90%). HRMS (ESI) *m*/*z* calcd for $C_{87}H_{124}N_2O_{22}$ ([M + Na]$^+$) 1571.8538, found 1571.8532; ^{1}H NMR ($CDCl_3$, 300 MHz, representative data) δ 8.15 (s, 1H), 6.82 (br, 1H), 6.44−5.83 (m, 6H), 5.56−5.10 (m, 9H), 4.86−4.16 (m, 5H), 3.97−3.11 (m, 23H), 2.80−2.24 (m, 13H); ^{13}C NMR ($CDCl_3$, 100 MHz, representative data) δ 216.0, 207.6, 192.5, 179.0, 173.5, 173.2, 169.8, 169.3, 165.8, 150.6, 140.7, 139.3, 137.6, 136.1, 135.8, 133.4, 130.0, 129.3, 127.1, 126.6, 119.4, 98.5, 89.2, 84.9, 84.4, 82.5, 80.2, 77.2, 75.8, 73.1, 73.0, 69.3, 67.2, 59.4, 59.3, 55.9, 51.3, 49.4, 46.6, 44.4, 44.2, 43.0, 42.8, 41.5, 41.4, 40.8, 40.2, 38.7, 38.5, 35.1, 34.6, 34.3, 33.8, 33.7, 33.2, 32.0, 31.6, 31.4, 31.3, 30.3, 28.8, 28.7, 27.8, 27.3, 27.0, 27.0, 25.3, 24.8, 24.3, 21.5, 21.2, 20.6, 16.3, 16.0, 15.8, 13.8, 13.4, 13.1, 12.8, 10.2.

1*E*,4*S*,4a*R*,5*R*,6a*S*,7*S*)-5-Acetyloxy-1-({[3-(dimethylamino)-propyl](methyl)amino}methylene)-11-hydroxy-4-(methoxymethyl)-4a,6a-dimethyl-2,10-dioxo-1,2,4,4a,5,6,6a,7,8,9,9a,10-dodecahydroindeno[4,5-*h*]isochromen-7-yl-*trans*-4-{(2*R*)-2-[(3*S*,6*R*,7*E*,9*R*,10*R*,12*R*,14*S*,15*E*,17*E*,19*E*,21*S*,23*S*,26*R*,27*R*,34a*S*)-9,27-dihydroxy-10,21-dimethoxy-6,8,12,14,20,26-hexamethyl-1,5,11,28,29-pentaoxo-1,4,5,6,9,10,11,12,13,14,21,22,23,24,25,26,27,28,29,31,32,33,34,34a-tetracosahydro-3*H*-23,27-epoxypyrido[2,1-*c*][1,4]oxazacyclohentriacontin-3-yl]propyl}cyclohexyl Octanedioate (8b). A solution of 41-desmethoxyrapamycin−suberate−wortmannin conjugate **6** (552 mg, 0.38 mmol) in TBME (15 mL) was cooled to −30 °C. *N*,*N*,*N*′-Trimethyl-1,3-propanediamine (51 mg, 0.44 mmol) in TBME (3 mL) was added dropwise over 10 min. After addition, the mixture was stirred at −30 °C for 1 h, then warmed to −20 °C and stirred for another 1 h. Hexane (20 mL) was introduced while maintaining the temperature at −15 to −20 °C. The product **8b** was collected on a Buchner funnel as a yellow powder (550 mg, 92%). HRMS (ESI) *m*/*z* calcd for $C_{87}H_{130}N_3O_{22}$ ([M + H]$^+$) 1568.9140, found 1568.9128; ^{1}H NMR ($CDCl_3$, 300 MHz, representative data) δ 8.15 (s, 1H), 6.44−5.85 (m, 5H), 5.56−5.11 (m, 4H), 4.86−4.16 (m, 5H), 3.88−3.10 (m, 23H), 2.80−2.22 (m, 28H); ^{13}C NMR ($CDCl_3$, 100 MHz, representative data) δ 215.3, 208.3, 192.6, 179.1, 173.6, 173.2, 169.9, 169.2, 166.8, 149.9, 140.1, 138.6, 137.7, 136.1, 135.6, 133.6, 130.2, 129.6, 126.6, 126.4, 98.5, 88.3, 84.9, 84.3, 82.6, 80.3, 77.2, 75.7, 73.2, 73.0, 69.2, 67.1, 59.4, 59.4, 59.2, 58.5, 55.9, 51.3, 46.6, 45.3, 44.4, 44.2, 43.0, 42.7, 41.6, 41.5, 40.8, 40.2, 38.9, 38.5, 35.1, 34.6, 34.3, 33.8, 33.7, 33.2, 32.0, 31.6, 31.4, 31.2, 30.3, 28.8, 28.7, 27.8, 27.3, 27.0, 25.7, 25.3, 24.8, 24.3, 21.5, 21.2, 20.6, 16.3, 16.0, 15.9, 15.8, 13.8, 13.4, 13.1, 10.2.

Acknowledgment. We thank George Morton for NMR data, Dr. Xidong Feng for HRMS data, Dr. Mark Tischler for solubility analyses, and Jessica Lucas for biomarker studies.

Supporting Information Available: Additional details of experimental procedures, representative ^{1}H, ^{13}C NMR, MS, and HPLC traces, and additional methods for stability studies.

This material is available free of charge via the Internet at http://pubs.acs.org.

References

(1) Hudes, G.; Carducci, M.; Tomczak, P.; Dutcher, J.; Figlin, R.; Kapoor, A.; Staroslawska, E.; Sosman, J.; McDermott, D.; Bodrogi, I.; Kovacevic, Z.; Lesovoy, V.; Schmidt-Wolf, I. G. H.; Barbarash, O.; Gokmen, E.; O'Toole, T.; Lustgarten, S.; Moore, L.; Motzer, R. J. Temsirolimus, interferon alfa, or both for advanced renal-cell carcinoma. *N. Engl. J. Med.* **2007**, *356*, 2271–2281.

(2) Motzer, R. J.; Escudier, B.; Oudard, S.; Hutson, T. E.; Porta, C.; Bracarda, S.; Grunwald, V.; Thompson, J. A.; Figlin, R. A.; Hollaender, N.; Urbanowitz, G.; Berg, W. J.; Kay, A.; Lebwohl, D.; Ravaud, A. Efficacy of everolimus in advanced renal cell carcinoma: a double-blind, randomized, placebo-controlled phase III trial. *Lancet* **2008**, *372*, 449–456.

(3) Carracedo, A.; Pandolfi, P. P. The PTEN-PI3K pathway: of feedbacks and cross-talks. *Oncogene* **2008**, *27*, 5527–5541.

(4) Guertin, D. A.; Sabatini, D. M. The pharmacology of mTOR inhibition. *Sci. Signaling* **2009**, *2*, No. pe24.

(5) Meric-Bernstam, F.; Gonzalez-Angulo, A. M. Targeting the mTOR signaling network for cancer therapy. *J. Clin. Oncol.* **2009**, *27*, 2278–2287.

(6) Sun, S.-Y.; Rosenberg, L. M.; Wang, X.; Zhou, Z.; Yue, P.; Fu, H.; Khuri, F. R. Activation of Akt and eIF4E survival pathways by rapamycin-mediated mammalian target of rapamycin inhibition. *Cancer Res.* **2005**, *65*, 7052–7058.

(7) Shi, Y.; Yan, H.; Frost, P.; Gera, J.; Lichtenstein, A. Mammalian target of rapamycin inhibitors activate the AKT kinase in multiple myeloma cells by up-regulating the insulin-like growth factor receptor/insulin receptor substrate-1/phosphatidylinositol 3-kinase cascade. *Mol. Cancer Ther.* **2005**, *4*, 1533–1540.

(8) Vlahos, C. J.; Matter, W. F.; Hui, K. Y.; Brown, R. F. A specific inhibitor of phosphatidylinositol 3-kinase, 2-(4-morpholinyl)-8-phenyl-4*H*-1-benzopyran-4-one (LY294002). *J. Biol. Chem.* **1994**, *269*, 5241–5248.

(9) Norman, B. H.; Shih, C.; Toth, J. E.; Ray, J. E.; Dodge, J. A.; Johnson, D. W.; Rutherford, P. G.; Schulz, R. M.; Worzalla, J. F.; Vlahos, C. J. Studies on the mechanism of phosphatidylinositol 3-kinase inhibition by wortmannin and related analogs. *J. Med. Chem.* **1996**, *39*, 1106–1111.

(10) Wang, X.; Yue, P.; Kim, Y. A.; Fu, H.; Khuri, F. R.; Sun, S.-Y. Enhancing mammalian target of rapamycin (mTOR)-targeted cancer therapy by preventing mTOR/raptor inhibition-initiated, mTOR/rictor-independent Akt activation. *Cancer Res.* **2008**, *68*, 7409–7418.

(11) O'Reilly, K. E.; Rojo, F.; She, Q.-B.; Solit, D.; Mills, G. B.; Smith, D.; Lane, H.; Hofmann, F.; Hicklin, D. J.; Ludwig, D. L.; Baselga, J.; Rosen, N. mTOR inhibition induces upstream receptor tyrosine kinase signaling and activates Akt. *Cancer Res.* **2006**, *66*, 1500–1508.

(12) Cloughesy, T. F.; Yoshimoto, K.; Nghiemphu, P.; Brown, K.; Dang, J.; Zhu, S.; Hseuh, T.; Chen, Y.; Wang, W.; Youngkin, D.; Liau, L.; Martin, N.; Becker, D.; Bergsneider, M.; Lai, A.; Green, R.; Oglesby, T.; Koleto, M.; Trent, J.; Horvath, S.; Mischel, P. S.; Mellinghoff, I. K.; Sawyers, C. L. Antitumor activity of rapamycin in a phase I trial for patients with recurrent PTEN-deficient glioblastoma. *PloS Med.* **2008**, *5*, 139–151.

(13) Yu, K.; Lucas, J.; Zhu, T.; Zask, A.; Gaydos, C.; Toral-Barzar, L.; Gu, J.; Li, F.; Chaudhary, I.; Cai, P.; Lotvin, J.; Petersen, R.; Ruppen, M.; Fawzi, M.; Ayral-Kaloustian, S.; Skotnicki, J.; Mansour, T.; Frost, P.; Gibbons, J. PWT-458, a novel pegylated-17-hydroxywortmannin, inhibits phosphatidylinositol 3-kinase signaling and suppresses growth of solid tumors. *Cancer Biol. Ther.* **2005**, *4*, 538–545.

(14) Ihle, N. T.; Williams, R.; Chow, S.; Chew, W.; Berggren, M. I.; Paine-Murrieta, G.; Minion, D. J.; Halter, R. J.; Wipf, P.; Abraham, R.; Kirkpatrick, L.; Powis, G. Molecular pharmacology and antitumor activity of PX-866, a novel inhibitor of phosphoinositide-3-kinase signaling. *Mol. Cancer Ther.* **2004**, 1535–7163.

(15) Wipf, P.; Minion, D. J.; Halter, R. J.; Berggren, M. I.; Ho, C. B.; Chiang, G. G.; Kirkpatrick, L.; Abraham, R.; Powls, G. Synthesis and biological evaluation of synthetic viridins derived from C(20)-heteroalkylation of the steroidal PI-3-kinase inhibitor wortmannin. *Org. Biomol. Chem.* **2004**, *2*, 1911–1920.

(16) Zhu, T.; Gu, J.; Yu, K.; Lucas, J.; Cai, P.; Tsao, R.; Gong, Y.; Li, F.; Chaudhary, I.; Desai, P.; Ruppen, M.; Fawzi, M.; Gibbons, J.; Ayral-Kaloustian, S.; Skotnicki, J.; Mansour, T.; Zask, A. Pegylated wortmannin and 17-hydroxywortmannin conjugates as phosphoinositide 3-kinase inhibitors active in human tumor xenograft models. *J. Med. Chem.* **2006**, *49*, 1373–1378.

(17) Zask, A.; Kaplan, J.; Toral-Barza, L.; Hollander, I.; Young, M.; Tischler, M.; Gaydos, C.; Cinque, M.; Lucas, J.; Yu, K. Synthesis and structure−activity relationships of ring-opened 17-hydroxywortmannins: potent phosphoinositide 3-kinase inhibitors with improved properties and anticancer efficacy. *J. Med. Chem.* **2008**, *51*, 1319–1323.

(18) Eng, C. P.; Sehgal, S. N.; Vezina, C. Activity of rapamycin (AY-22,989) against transplanted tumors. *J. Antibiot.* **1984**, *37*, 1231.

(19) Goss, R. M.; Lanceron, S. E.; Wise, N. J.; Moss, S. J. Generating rapamycin analogues by directed biosynthesis: starter acid substrate specificity of mono-substituted cyclohexane carboxylic acids. *Org. Biomol. Chem.* **2006**, *4*, 4071–4073.

(20) Graziani, E. I. Recent advances in the chemistry, biosynthesis and pharmacology of rapamycin analogs. *Nat. Prod. Rep.* **2009**, *26*, 602–609.

(21) Compound **9b** (17-OH-PX-866) was prepared from **2a**, according to the method of ref 17 and had in vitro activity comparable to that of PX-866, which in our PI3Kα enzyme assay was considerably less potent (IC_{50} = 88 nM)[17] than what was reported in the literature.[15]

(22) Ogawa, Y.; Kodaka, M.; Okuno, H. Trigger lipids inducing pH-dependent liposome fusion. *Chem. Phys. Lipids* **2002**, *119*, 51–68.

(23) Rapamycin 31-trimethylsilyl ether may be synthesized according to the procedure described in the following patent: Shaw, C.-C.; Sellstedt, J.; Noureldin, R.; Cheal, G. K.; Fortier, G. Regioselective Synthesis of Rapamycin Derivatives. U.S. Patent 6,277,983, **2001**.

(24) Simamora, P.; Alvarez, J. M.; Yalkowsky, S. H. Solubilization of rapamycin. *Int. J. Pharm.* **2001**, *213*, 25–29.

(25) Morphy, R.; Rankovic, Z. Designed multiple ligands. An emerging drug discovery paradigm. *J. Med. Chem.* **2005**, *48*, 6523–6543.

(26) Meunier, B. Hybrid molecules with a dual mode of action: dream or reality? *Acc. Chem. Res.* **2008**, *41*, 69–77.

(27) Findlay, J. A.; Radics, L. On the chemistry and high field nuclear magnetic resonance spectroscopy of rapamycin. *Can. J. Chem.* **1980**, *58*, 579–590.

(28) Hughes, P.; Musser, J.; Conklin, M.; Russo, R. The isolation, synthesis and characterization of an isomeric form of rapamycin. *Tetrahedron Lett.* **1992**, *33*, 4739–4742.